Measurement report: Long emission-wavelength chromophores dominate the light absorption of brown carbon in Aerosols over Bangkok: impact from biomass burning

Jiao Tang[1,2,3], Jiaqi Wang[1,2,3,7], Guangcai Zhong[1,2,3], Hongxing Jiang[1,2,3,7], Yangzhi Mo[1,2,3], Bolong Zhang[1,2,3,7], Xiaofei Geng[1,2,3,7], Yingjun Chen[4], Jianhui Tang[5], Congguo Tian[5], Surat Bualert[6], Jun Li[1,2,3], Gan Zhang[1,2,3]

[1]State Key Laboratory of Organic Geochemistry and Guangdong Key Laboratory of Environmental Protection and Resources Utilization, Guangzhou Institute of Geochemistry, Chinese Academy of Sciences, Guangzhou 510640, China

[2]CAS Center for Excellence in Deep Earth Science, Guangzhou, 510640, China

[3]Joint Laboratory of the Guangdong-Hong Kong-Macao Greater Bay Area for the Environment, Guangzhou Institute of Geochemistry, Chinese Academy of Sciences, Guangzhou 510640, China

[4]Department of Environmental Science and Engineering, Fudan University, Shanghai 200092, P.R. China

[5]Key Laboratory of Coastal Environmental Processes and Ecological Remediation, Yantai Institute of Coastal Zone Research, Chinese Academy of Sciences, Yantai 264003, China

[6]Faculty of Environment, Kasetsart University, Bangkok, 10900, Thailand

[7]University of Chinese Academy of Sciences, Beijing 100049, China

Correspondence: Guangcai Zhong (gczhong@gig.ac.cn)

Abstract: Chromophores represent an important portion of light-absorbing species, i.e. brown carbon. Yet knowledge on what and how chromophores contribute to aerosol light absorption is still sparse. To address this problem, we examined soluble independent chromophores in a set of year-round aerosol samples from Bangkok. The water-soluble fluorescent chromophores identified via excitation-emission matrix (EEM) spectroscopy and follow-up parallel factor analysis could be mainly assigned as humic-like substances and protein-like substances, which differed in their EEM pattern from that of the methanol-soluble fraction. The emission wavelength of fluorescent chromophores in environmental samples tended to increase compared with that of the primary combustion emission, which could be attributed to secondary formation or the aging process. Fluorescent indices inferred that these light-absorbing chromophores were not significantly humified and comprised a mixture of organic matter of terrestrial and microbial origin, which exhibited a different characteristic from primary biomass burning and coal combustion results. A multiple linear regression analysis revealed that larger fluorescent chromophores that were oxygen-rich and highly aromatic with high molecular weights, were the key contributors of light absorption, preferably at longer emission wavelength (λ_{max} > 500 nm). Positive matrix factorization analysis further suggested that up to 50% of these responsible chromophores originated from biomass burning emissions.

1. Introduction

Atmospheric aerosols play a substantial role in climate change through radiative forcing (Alexander et al., 2008). Carbonaceous aerosols mainly include organic carbon (OC) and elemental carbon (EC). Brown carbon (BrC) is a specific type of OC that absorbs radiation efficiently in the near-ultraviolet and visible (UV-vis) range (Laskin et al., 2015;Kirchstetter et al., 2004) and may contribute 15% or more of total light absorption over the UV-vis spectrum (Kirchstetter and Thatcher, 2012;Liu et al., 2013). This fraction can significantly affect atmospheric chemistry, air quality, and climate change (Marrero-Ortiz et al., 2018;Laskin et al., 2015). Forest fires, residential heating by wood and coal, biogenic release, and secondary formation contribute to BrC in the atmosphere (Laskin et al., 2015). Many studies have indicated that the optical properties of BrC may significantly evolve as a result of atmospheric processes such as oxidation (Fan et al., 2020), solar irradiation (Wong et al., 2017), and relative humidity (Kasthuriarachchi et al., 2020). These factors cause variability in the chemical compositions and levels of BrC across source regions and receptors, resulting in a high degree of uncertainty regarding the effects of BrC (Dasari et al., 2019;Xie et al., 2019).

Light absorption of BrC is associated with its molecular composition and chemical structure (Song et al., 2019;Lin et al., 2018;Mo et al., 2018;Jiang et al., 2020). Detailed structural characterization of BrC compounds is essential to understand their sources and chemical processes in the atmosphere. High-resolution mass spectrometry (HRMS) is a powerful tool for molecular-level chemical analysis of organic aerosols (Laskin et al., 2018). Combinations of offline high-performance liquid chromatography (HPLC), a photodiode array detector, and HRMS allow the chemical characterization of aerosols specific to BrC (Lin et al., 2018;Lin et al., 2016;Lin et al., 2015;Lin et al., 2017). With these combination approaches, nitroaromatics, aromatic acids, phenols, polycyclic aromatic hydrocarbons and their derivatives are basically identified as BrC chromophores (Wang et al., 2020b;Yan et al., 2020). However, it should be noted that it is difficult to ionize some organic compounds for detection using HRMS, and even for those that can be detected, HRMS can only provide possible molecular structures based on empirical deduction (Song et al., 2018;Lin et al., 2015). The isomeric complexity of natural organic matter may have exceeded achievable one-dimensional chromatographic resolution (Hawkes et al., 2018), and therefore, the majority of components in the BrC mixture remain undetermined.

Excitation-emission matrix (EEM) fluorescence spectroscopy detects bulk chromophores in a solution (Chen et al., 2016b). Chromophores can be revealed by EEM with information on their chemical structures associated with molecular weight, aromatic rings, conjugated systems, etc (Wu et al., 2003). For example, a redshift in emission spectral maxima can be caused by an increase in the

number of aromatic rings condensed in a straight chain, conjugated double bonds, or formational changes that permit vibrational energy losses of the promoted electrons (Wu et al., 2003). A significant Stokes shift with emission wavelength can be observed in aged secondary organic aerosols (SOA) using EEM spectroscopy (Lee et al., 2013). Parallel factor (PARAFAC) analysis has been widely used to decompose the EEM spectral signature into independent underlying components (Han et al., 2020;Yue et al., 2019;Wu et al., 2019;Chen et al., 2019b), adding valuable information to absorbance-based measurements (Yan and Kim, 2017). This technique helps to categorize groups of similar fluorophores or chromophores or similar optical properties, thereby allowing a better understanding of the chemical properties of BrC, while it should be noted that not all chromophores in BrC compounds are fluorescence (Chen et al., 2019a). There is evidence that BrC absorption is closely correlated with fluorescent chromophores (Huo et al., 2018). However, the intrinsic relationship between fluorescent chromophores and BrC absorption has not been explored.

Southeast Asia is subject to intensive regional biomass burning, the emissions from which may contribute to atmospheric brown clouds (Ramanathan et al., 2007;Laskin et al., 2015). The contribution of biomass burning to aerosol optical depth was evaluated to be more than 56% over this region (Huang et al., 2013). Despite many studies focused on the characterization of atmospheric black carbon (BC) (See et al., 2006;Fujii et al., 2014;Permadi et al., 2018), studies on BrC in the region are still limited. A recent study in Singapore indicated that water-soluble OC (WSOC) exhibited strong wavelength dependence and even higher values of BrC absorption than those from Korea, India, China, and Nepal (Adam et al., 2020), indicating abundant water-soluble BrC in the air over Southeast Asia.

This study was performed to explore the relationships between EEM chromophores and BrC light absorption in soluble aerosol organic matter. A set of year-round aerosol samples from Bangkok, Thailand, was analyzed. Water-soluble and methanol-soluble BrC in the aerosol samples were characterized by EEM followed by statistical analyses to retrieve information on the contributions of fluorescent chromophores to BrC light absorption, as well as their emission sources. This study provides a comprehensive dataset on seasonal variability in the light absorption properties, sources, and chemical components of BrC, which may be useful for improving further modeling and field observation.

2. Experiment

2.1. Sample Collection and Extraction.

Eighty-five total suspended particulate (TSP) samples were collected on the roof (57 m above ground level) of the Faculty of Environment, Kasetsart University (100°57′ E and 13°85′ N) in Bangkok, Thailand (Fig. S1). Detailed information about the sampling site is presented elsewhere

(Wang et al., 2020a). Sampling was performed from January 18, 2016 to January 28, 2017, and the sampling period was divided into four seasons: the pre-hot season (January 18–February 28, 2016), hot season (March 2–May 30, 2016), monsoon (June 2–October 30, 2016), and cool season (November 1, 2016–January 28, 2017). Table S1 lists the average meteorological data in the four seasons. Generally, during the sampling period, the hot season was characterized by high temperatures and wind speeds, and the monsoon season by high humidity. TSP samples were collected over 24 h using a high-volume (0.3 m^3 min^{-1}) sampler with quartz-fiber filters (QFFs, prebaked for 6 h at 450 °C). All samples and field blanks were stored under dark conditions at –20 °C until analysis.

WSOC was prepared by ultrasonication extraction of filter punches with ultra-pure deionized water (resistivity of > 18.2 MΩ). The methanol-soluble OC (MSOC) fraction was then obtained by extracting the freeze-dried residue on the same QFFs after water extraction with HPLC-grade methanol, which is used for water-insoluble fractions (Chen and Bond, 2010). It is worth noting that the MSOC in this study is not necessarily like that of the same name in other studies. The extract solutions were passed through 0.22-μm PTFE filters and subjected to follow-up UV-vis absorption and fluorescence spectral analysis. The mass concentrations of WSOC and MSOC were measured, and the method are shown in the Supplement.

2.2. Absorption Spectra and Fluorescence Spectra.

The extract solutions were placed in quartz cells with a path-length of 1 cm and subjected to analysis using an fluorometer (Aqualog; Horiba Scientific, USA). Absorption spectra and EEM spectra were obtained simultaneously using this instrument. The contribution of solvents was subtracted from the extract spectra. UV-vis absorption spectra were scanned in the range of 239 to 800 nm with a step size of 3 nm. The Fluorescence spectra were recorded with emission wavelength (Em) ranging from 247.01 to 825.03 nm and excitation wavelength (Ex) ranging from 239 to 800 nm. The wavelength increments of the scans for Em and Ex were 4.66 and 3 nm, respectively. The calculation of optical parameters and the relative contributions of BrC to total aerosol light absorption are presented in the Supplement.

2.3. Factor analysis

In this study, we built a PARAFAC model, based on 85 TSP sample fluorescence (samples × Ex × Em: 85 × 188 × 125, 85-model). Original EEM spectra were corrected and decomposed via PARAFAC analysis with reference to earlier methods using drEEM toolbox version 2.0 with MATLAB software (http://models.life.ku.dk/drEEM, last access: June 2014) (Murphy et al., 2013;Andersson and Bro, 2000). The absorbance, all below 1 at 239 nm, was deemed suitable for correcting the EEM

spectra for inner filter effects (IFEs) (Luciani et al., 2009;Gu and Kenny, 2009;Fu et al., 2015), and the sample EEM spectra, and blanks were normalized relative to the Raman peak area of ultrapure deionized water collected on the same day to correct fluorescence in Raman Units (RU) (Murphy et al., 2013;Murphy et al., 2010). Spectra with Em > 580 nm and Ex < 250 nm were removed to eliminate noisy data. The non-negativity constraint is necessary to obtain reasonable spectra, and signals of first-order Rayleigh, Raman, and second-order Rayleigh scattering in the EEM spectra were removed using the interpolation method (Bahram et al., 2006). The two- to nine-component PARAFAC model was explored, within the context of spectral loading, core consistency, and residual analysis (Figs. S2–S5). Finally, seven and six components were identified in the WSOC and MSOC fractions, which explained 99.89% and 99.76% of the variance, respectively. Both the seven- and six-component PARAFAC solutions passed the split-half analysis with the split style of "$S_4C_6T_3$", and residuals were examined to ensure that there was no systematic variation. The parameters obtained from the PARAFAC model were used to calculate the approximate abundance of each component, expressed as F_{max} (in RU), corresponding to the maximum fluorescence intensity for a particular sample.

Fluorescence indices based on intensity ratios that provide insight into the origins of dissolved BrC, such as the humification index (HIX) (the ratio of average emission intensity in the 435−480-nm range to that in the 300−345-nm range following excitation at 254 nm, which was used to reflect the degree of humification) (Zsolnay et al., 1999), the biological index (BIX) (the ratio of emission intensities at 380 and 430 nm following excitation at 310 nm, reflecting autochthonous biological activity in water samples) (Huguet et al., 2009), and fluorescence index (FI) (the ratio of emission intensities at 470 and 520 nm following excitation at 370 nm, reflecting the possibility of microbial origin and for examining differences in precursor organic materials) (Lee et al., 2013;Murphy et al., 2018).

2.4. Statistical analysis

A hierarchical cluster method was used to classify aerosol samples based on the relative contributions of PARAFAC components to the respective samples. The Squared Euclidean distance method was used to evaluate the distances between samples, and the Between-group linkage method was chosen for hierarchical cluster analysis. The multiple linear regression (MLR) model was applied to elucidate the relationship between fluorescent chromophores and light absorption of BrC using a stepwise screening process. Analyses were performed using SPSS software (SPSS Inc., Chicago, IL, USA).

3. Results and Discussion

3.1. EEM of dissolved organic substances.

Fluorescence spectra coupled with PARAFAC results can provide more information about the chemical structures of chromophores. Figure 1 and Table S2 show the seven-component (P1–7) PARAFAC solutions of WSOC in the samples of aerosol over Bangkok, the peaks of which fell mainly into the humic-like and protein-like chromophore regions in the plots. Components P2, P3, P4, and P6 were identified as humic-like substances (HULIS) (Chen et al., 2017a;Stedmon and Markager, 2005;Wu et al., 2019;Chen et al., 2003). A second peak was observed at a high excitation wavelength for these components, indicating the existence of a large number of condensed aromatic moieties, conjugated bonds, and nonlinear ring systems (Matos et al., 2015). Among them, P2, P3, and P4 had a longer emission wavelength (> 400 nm) than P6, likely due to the low probability of fluorescence emission from quinonoid n-π^* transitions (Cory and McKnight, 2005). P3 produced similar spectra to those of aqueous reaction products of hydroxyacetone with glycine (Gao and Zhang, 2018), and dissolved organic matter (DOM) in the surface water of Xiangxi Bay and Three Gorges Reservoir (Wang et al., 2019). P6 had a peak similar to those in the fluorescence spectra of N-containing SOA species formed by α-pinene under ozonolysis and photooxidation with NH_3 in a flow reactor (Babar et al., 2017) as well as pyridoxine (Pohlker et al., 2012), indicating a possible biological source. P5 was similar to a previously identified fluorophore in $PM_{2.5}$ from Xi'an (Chen et al., 2019b). P1 and P7 could be assigned as protein-like organic matter (PLOM) due to their short emission wavelengths (Wu et al., 2003). Specifically, P7 resembled a tyrosine-like fluorophore (Zhou et al., 2019;Chen et al., 2003) and may be related to non-N-containing species (Chen et al., 2016b).

The MSOC fraction extracted from the filter residue after water extraction produced fluorescence signals with fluorescence patterns different from those of the WSOC fraction, indicating a different chemical composition from that of WSOC. Thus, WSOC with the addition of MSOC may provide a more comprehensive description of the optical and chemical characteristics of BrC compared to WSOC alone. Six components (C1–C6) were resolved for the MSOC. Among them, C1 and C2 were associated with shorter excitation wavelengths (< 250 nm) but longer emission wavelengths (> 380 nm), indicating the presence of fulvic-like substances (Chen et al., 2003;Mounier et al., 1999). C6 produced a pattern similar to that of tyrosine-like fluorescence (Stedmon and Markager, 2005). Although C4 had a similar EEM spectrum as P4 of WSOC, the two components were chemically different in polarity, suggesting different behaviors in the environment (Ishii and Boyer, 2012). Note that there were no special chemical structures for the different types of chromophores, and therefore, the origins and chemical structures of HULIS and PLOM studied here are not necessarily like those with the same names in other types of organic matter.

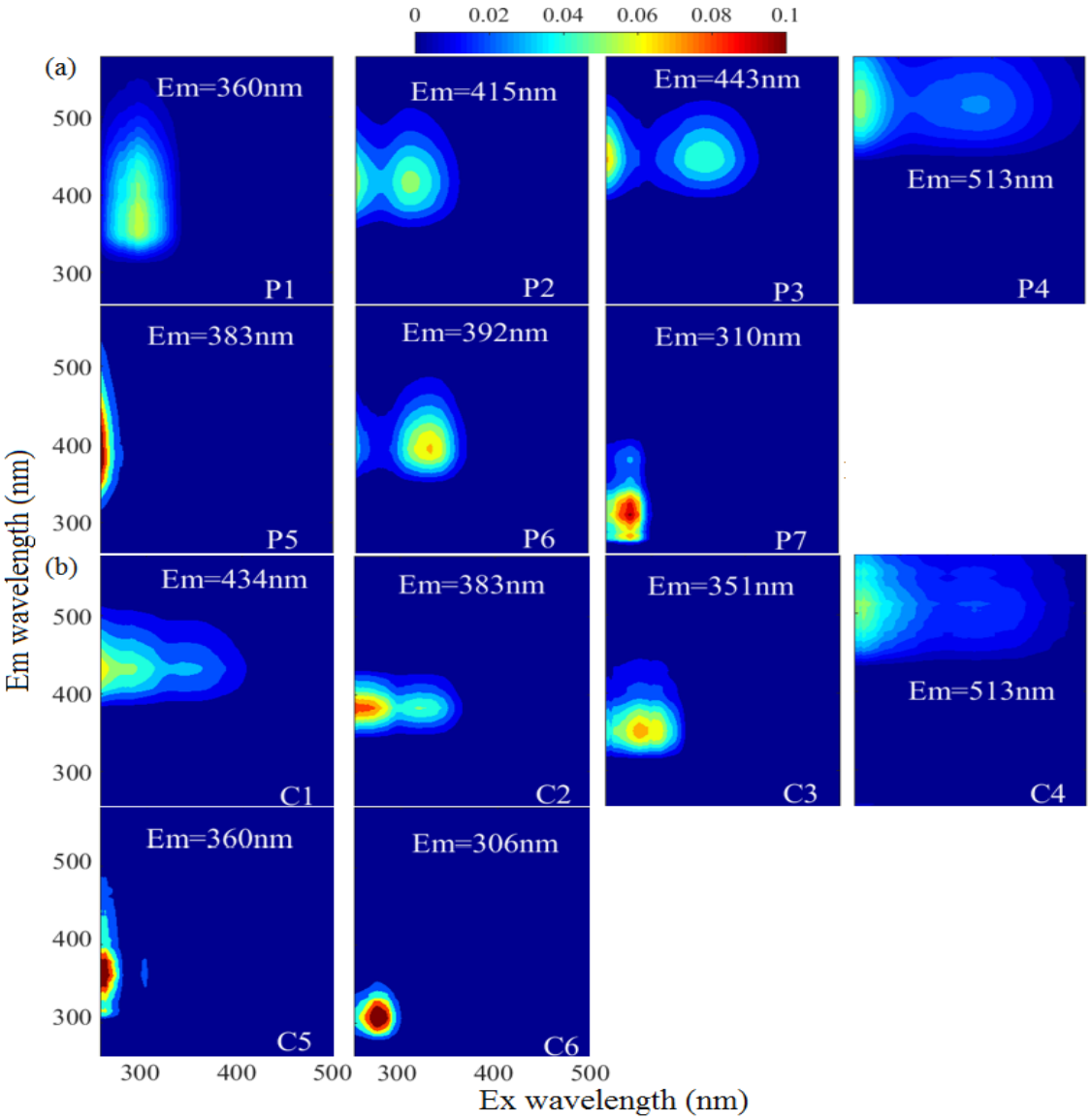

Figure 1. The fluorescent components identified by the PARAFAC (parallel factor) analysis for EEM of water-soluble organic carbon (P1–P7, WSOC, a) and methanol-soluble organic carbon (C1–C6, MSOC, b) in the aerosol samples over Bangkok in Thailand (n=85). The color represents that the intensity was normalized to set the maximum as 0.1.

To further explore the potential sources of the EEM-PARAFAC components, we added 60 source samples to the matrices. The source sample EEM data were described in our previous study (Tang et al., 2020b), including those of 33 biomass-burning samples (IDs: 1–33), 17 coal-combustion samples (IDs: 34–50) samples, eight tunnel samples (IDs: 51–58) and two vehicle-exhaust samples from trucks (IDs: 59–60) , which are important sources of BrC in the atmosphere. This, in combination with our Bangkok field samples, yielded a new matrix (145 × 188 × 125, 145-model) for modeling. PARAFAC analysis successfully decomposed the dataset, and the output was the same as for the 85-model. The component solutions are presented in Fig. S6. To validate the stability of the model after loading by the new matrix, the Tucker congruence coefficient (TCC) was calculated to determine the similarity

of two fluorescence spectra between the two models (refer to Text S3 of Supplement). Note that a higher TCC value would indicate a higher degree of similarity of the spectra. As shown in Table S2 and Fig. S7, high TCC values were found as expected between the 85-model components and the 145-model components, indicating that the two models identified similar fluorescent chromophores. It should be noted that one additional fluorescent component was identified each for the WSOC and MSOC fractions in the new 145-model, respectively, but these components were only highly characterized by source emission samples, as reported in our previous study (Tang et al., 2020b).

Using the distribution proportions of the EEM-PARAFAC fitted components (145-model), we conducted hierarchical cluster analysis of the mixed ambient and source samples. The results are shown in Figs. S9 and S10. For the WSOC fraction, all aerosol samples from Bangkok and tunnel samples were assigned to cluster A, whereas biomass-burning and coal-combustion aerosols were assigned to clusters C and D, respectively. This implied that the fluorescent chromophore types could be somewhat related to the emission precursors of the aerosol components. However, the distribution of fluorescent chromophores varied clearly between the ambient aerosols and source samples. The ambient aerosol samples contained higher levels of fluorescent chromophores with longer emission wavelengths that were related to humic-like or fulvic-like chromophores (components 145M-P1 (P1 component in 145-model), 145M-P5, and 145M-P6), whereas the primary biomass-burning and coal-combustion samples contained high-intensity fluorescent chromophores with shorter emission wavelengths that were related to protein-like fluorescence (145M-P2 and 145M-P4). These phenomena was similarly reported previously, i.e., protein-like substances produce compounds with similar fluorescence properties as humic substances under irradiation conditions (Bianco et al., 2014). Similar differences between field samples and source samples were found for the MSOC fraction. Therefore, our results confirmed that chemical reactions or “aging” in the atmosphere greatly modifies the chromophore patterns of emission sources by both bleaching the source chromophores or producing new chromophores and, at least in this case, shifts the chromophore emission wavelength toward longer wavelengths, i.e., from protein-like to fulvic-like (Bianco et al., 2014;Bianco et al., 2016;Lee et al., 2013).

3.2. Fluorescence-derived indices

The ratios of fluorescence intensity from specific spectral regions of an EEM were used as indicators for the relative contributions of organic matter derived from terrestrial or microbial sources in natural waters (Shimabuku et al., 2017;Birdwell and Engel, 2010;Mcknight et al., 2001). HIX was initially introduced to estimate the degree of maturation of DOM in soil (Zsolnay et al., 1999), representing the degree of humification of organic matter, for which higher HIX values also indicate

higher degree of polycondensation (low H/C ratio) and aromaticity (Qin et al., 2018). Generally, high HIX values (> 10) correspond to strongly humified or aromatic organics, principally of terrestrial origin, whereas low values (< 4) are indicative of autochthonous or microbial origin. As shown in Table 1 and Fig. 2, the HIX values were 3.4±0.99 and 2.0±0.59 for WSOC and MSOC, respectively, in aerosol samples from Bangkok. All HIX values were less than 10, which could be viewed as a nominal cutoff below which DOM is not significantly humified (Birdwell and Valsaraj, 2010;Zsolnay et al., 1999;Huguet et al., 2009). Figure 2 shows the HIX values in primary biomass-burning and coal-combustion samples, which were much lower than those in the ambient samples, indicating that the lower values of HIX in the atmosphere likely correspond to freshly introduced material. Lee et al. (2013) reported that fresh SOA had low HIX values, but these values increased significantly upon aging with ammonia. The much higher HIX values in the WSOC compared to the MSOC suggest that WSOC may have a higher degree of aromaticity or a more condensed chemical structure. Our previous study revealed that MSOC has a higher molecular weight but lower aromaticity index than the corresponding WSOC in combustion experiment aerosol samples, indicating a more aliphatic structure in the MSOC (Tang et al., 2020b). The HIX values of WSOC were highest in the hot season (3.9±1.1), followed by the pre-hot season (3.3±1.1), cool season (2.9±0.36), and monsoon (2.5±0.22), whereas those of the MSOC tended to be higher in the hot and cool seasons than in the monsoon and pre-hot seasons. The HIX values in the WSOC fraction were comparable to those of water-soluble organic aerosols in the high Arctic atmosphere (mean: 2.9) (Fu et al., 2015) and higher than those of water-soluble aerosols (1.2±0.1 in winter and 2.0±0.3 in summer) over northwest China (Qin et al., 2018), likely indicating a higher degree of chromophore humification.

Table 1 Seasonal averages of the concentration of organic carbon (OC), elemental carbon (EC), water-soluble organic carbon (WSOC), and methanol-soluble organic carbon (MSOC), BrC absorption, fluorescence indices and levoglucosan level for aerosol samples collected from Bangkok in Thailand. Pre-hot season is from January 18 to February 29, 2016; hot season is from March 2 to May 31, 2016; monsoon is from June 2 to October 30, 2016; cool season is from November 1, 2016 to January 28, 2017.

	Annual (n=85) Ave ± sd	Pre-Hot season (n=7) Ave ± sd	Hot season (n=41) Ave ± sd	Monsoon (n=7) Ave ± sd	Cool season (n=30) Ave ± sd
[a]OC (μg C m^{-3})	12±7.3	19±9.3	9.6±6.7	6.5±0.97	16±5.6
[a]EC (μg C m^{-3})	1.4±0.48	2.0±0.45	1.2±0.47	1.2±0.15	1.5±0.40
[a]OC/EC	8.9±5.2	9.6±3.4	8.4±6.8	5.4±0.51	10±2.5
			WSOC		
μg C m^{-3}	6.2±4.2	9.9±5.7	5.3±4.1	2.6±0.31	7.4±3.4

AAE (330–400 nm)	5.1±0.68	5.0±0.52	5.4±0.56	6.2±0.11	4.5±0.34
Abs_{365} (Mm^{-1})	5.6±4.9	10±7.4	4.5±4.5	1.2±0.21	7.2±4.1
MAE_{365} (m^2 g^{-1} C)	0.83±0.25	0.96±0.19	0.78±0.23	0.45±0.06	0.95±0.21
FI	1.6±0.10	1.6±0.09	1.6±0.08	1.7±0.07	1.7±0.07
BIX	0.82±0.13	0.83±0.14	0.74±0.13	0.92±0.05	0.89±0.07
HIX	3.4±0.99	3.3±1.1	3.9±1.1	2.5±0.22	2.9±0.36
			MSOC		
μg C m^{-3}	6.0±3.4	9.2±4.0	4.3±2.9	3.9±0.86	8.1±2.6
AAE (330–400 nm)	5.2±0.94	4.9±0.69	5.5±1.1	5.1±0.15	4.7±0.55
Abs_{365} (Mm^{-1})	1.7±1.4	1.9±1.6	1.0±0.99	0.72±0.23	2.7±1.4
MAE_{365} (m^2 g^{-1} C)	0.26±0.12	0.19±0.08	0.23±0.11	0.19±0.06	0.33±0.11
FI	1.8±0.20	1.5±0.20	1.8±0.23	2.0±0.10	1.8±0.06
BIX	1.2±0.18	1.4±0.20	1.2±0.19	1.3±0.09	1.3±0.14
HIX	2.0±0.59	1.3±0.41	2.1±0.68	1.9±0.17	2.1±0.42
[a]Levoglucosan (ng C m^{-3})	222±485	362±438	185±654	42±16	280±185
[a]Levoglucosan/TSP ($\times 10^{-3}$)	2.9±2.9	3.4±3.1	2.3±3.6	1.9±0.98	3.9±1.8

a: described elsewhere (Wang et al., 2020a).

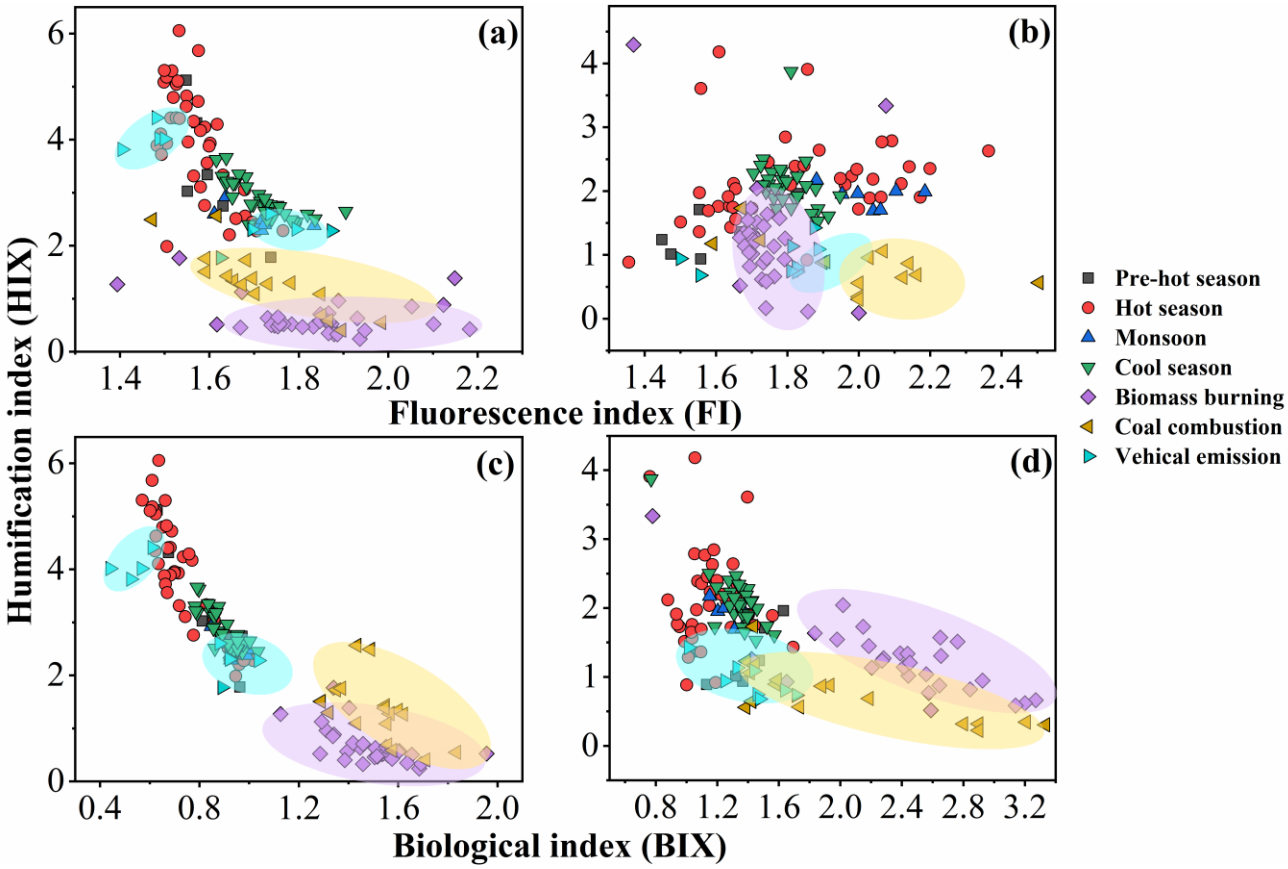

Figure 2. Fluorescence index (FI), biological index (BIX), and humification index (HIX) of water-soluble organic carbon (WSOC, a, c) and methanol-soluble organic carbon (MSOC, b, d) in aerosol samples from Bangkok, Thailand, as well as source emission samples including biomass burning, coal combustion and vehicle emission which were encircled by a violet, yellow, and blue region, respectively. Note that the fluorescence characteristic of source samples was described elsewhere (Tang et al., 2020b), but the fluorescence indices was first reported in this study. Pre-hot season is from January 18 to February 29, 2016; hot season is from March 2 to May 31, 2016; monsoon is from June 2 to October 30, 2016; cool season is from November 1, 2016 to January 28, 2017.

The BIX and FI were previously proposed as proxies for the contribution of biogenic organic matter and autochthonous biological activity in natural water, respectively (Fu et al., 2015;Qin et al., 2018). For example, the FI decreased by up to 20% indicating that the samples appeared increasingly like "terrestrial" DOM, whereas the BIX increased by up to 37% indicating that the samples became more "autochthonous" in character (Murphy et al., 2018;Gabor et al., 2014). FI values ≤ 1.4 correspond to terrestrially derived organics and higher aromaticity, whereas values ≥ 1.9 correspond to microbial sources and a lower aromatic carbon content (Mcknight et al., 2001). An increase in BIX is related to an increase in the contribution of microbially derived organics, with high values (> 1) shown to correspond to a predominantly biological or microbial origin of DOM and the presence of organic matter freshly released into water, whereas values ≤ 0.6 indicate the presence of little biological material (Huguet et al., 2009).

The FI and BIX values of the Bangkok aerosol samples are summarized in Table 1 and Fig. 2. The FI values of the WSOC and MSOC were 1.6±0.10 and 1.8±0.20, respectively, suggesting that these chromophores are representative of both terrestrially and microbially derived organic matter. The BIX values of the WSOC and MSOC were 0.82±0.13 and 1.2±0.18, respectively. Almost all BIX values were greater than 0.6 in the two fractions, suggesting biological or microbial contribution. Lee et al. (2013) reported that the BIX values of SOA samples averaged 0.6 and increased upon aging. In addition, the results of our source samples showed that primary biomass-burning and coal-combustion samples had high FI and BIX values (Fig. 2). These results indicate that these chromophores in Bangkok were likely freshly introduced or derived from biomass burning and coal combustion. Further, an increase in BIX in the MSOC in comparison with the WSOC was observed in primary biomass-burning and coal-combustion samples, consistent with the Bangkok samples. The BIX values were similar to those in the WSOC in Arctic aerosols (0.6–0.96, mean: 0.72), which were within the extreme values for the predominance of humic- or protein-like fluorophores (Fu et al., 2015). BIX values exhibited the opposite trend from HIX values, with low BIX values in the hot season. This may be explained by a previous study showing that a high BIX appears to indicate little humification (Birdwell and Engel, 2010). It should be noted that the fluorescence indices (FI, BIX, and HIX) were first applied for aquatic and soil organic compounds and further extended to the atmosphere due to the similarities in the properties of organic matter (Graber and Rudich, 2006). However, the values observed for primary biomass burning and coal combustion in this study differ from with the previously established fluorescence standards for aquatic environments and soil. Therefore, caution is required when using these indices to appoint source of atmospheric chromophores (Wu et al., 2021).

3.3. Optical properties of dissolved BrC.

Figure 3 shows the variations in soluble OC concentrations and the corresponding light absorption coefficient at 365 nm (Abs_{365}). In general, the Abs_{365} closely tracked the variations in the mass concentrations of WSOC and MSOC ($p < 0.000$, $R^2 = 0.95$ and $p < 0.000$, $R^2 = 0.75$, respectively) (Fig. S11), indicating that the portions of BrC in both fractions were considerably stable. Furthermore, light absorption at 365nm were higher in the pre-hot season, hot season, and cool season than that in the monsoon season. According to the levoglucosan level that generally regarded as biomass burning tracers and the ratios of levoglucosan/TSP (Table 1), we infer that the non-monsoon season were more affected by biomass burning and also showed high absorption.

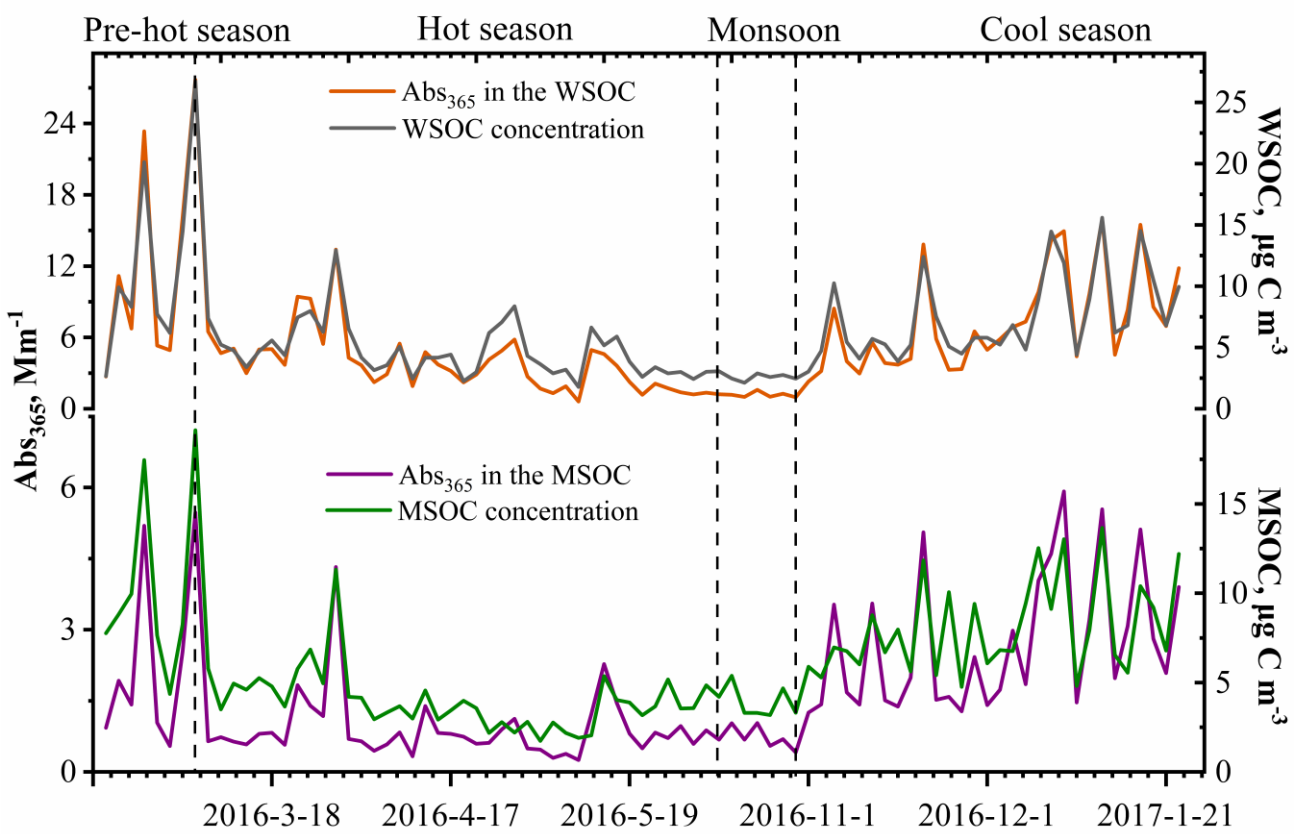

Figure 3. Time series plots of water-soluble organic carbon (WSOC) and methanol-soluble organic carbon (MSOC) concentration (μg C m^{-3}) and water- and methanol-extract light absorption coefficient at 365 nm (Abs_{365}) (Mm^{-1}) in the aerosol samples from Bangkok, Thailand during 2016–2017.

The absorption Ångström exponent (AAE) and mass absorption efficiency (MAE) are important optical parameters reflecting the spectral dependence and light absorption ability of BrC, respectively. The magnitude of the AAE reflects the differences in BrC source and atmospheric processes (Lack et al., 2013). Typically, the AAE value is close to 1 when light absorption is dominated by soot (Kirchstetter et al., 2004), roughly 1–3 for simulated biomass-burning aerosols (Hopkins et al., 2007), and up to 6–7 for water-soluble HULIS in biomass burning-impacted aerosols (Hoffer et al., 2006). The AAE values of the WSOC and MSOC between 330 and 400 nm in this study were up to 5.1±0.68 and 5.2±0.94 (Fig. 4), respectively, indicating strong wavelength dependence in the light absorption capability. These high values show that BrC tends to absorb more solar irradiation over ultraviolet wavelengths, which is comparable to BC absorption as shown in Fig. S12. These observations indicate that BrC has important impacts on photochemical reactions in the atmosphere (Barnard et al., 2008). The AAE values in this study are similar to those of water-soluble BrC over biomass burning-impacted regions, such as Beijing (Mo et al., 2018;Yan et al., 2015) and Guangzhou (Liu et al., 2018), but lower than those of aerosols from simulated biomass-burning and coal-combustion experiments (Fan et al., 2018;Tang et al., 2020a;Li et al., 2018). However, it should be noted that the BrC AAE varies in the

atmosphere. Dasari et al. (2019) reported that AAE values of water-soluble BrC increase continuously due to photolysis of chromophores and atmospheric oxidation during long-range transport over the Indo-Gangetic Plain (IGP). In addition, pH changes can cause the absorption spectra of some BrC species to shift to longer wavelengths upon deprotonation, decreasing AAE values (Mo et al., 2017). The pH values of WSOC fraction for all the samples were within the range of 5–7, generally thinking it didn't affect the absorbance according to a prior study (Chen et al., 2016a).

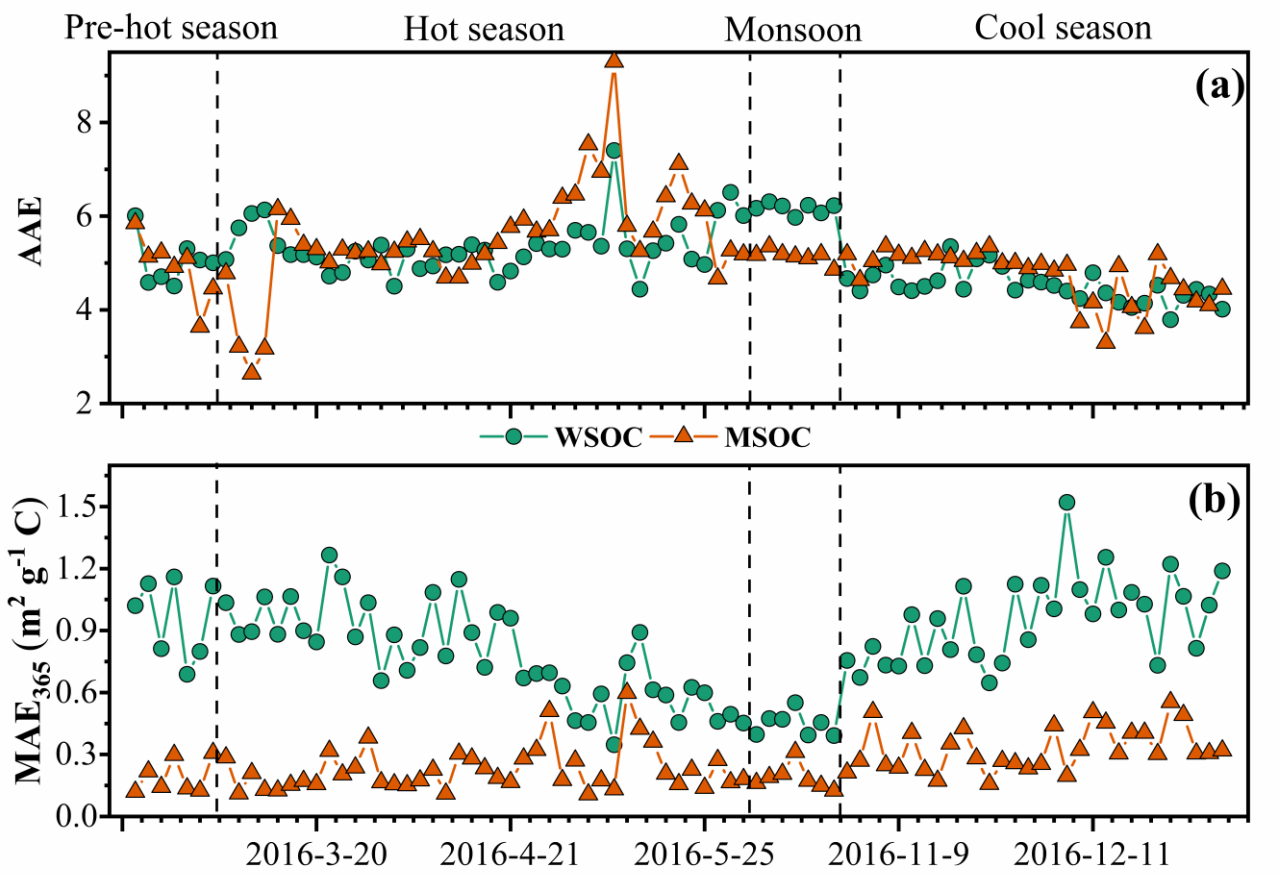

Figure 4. Time series plots of Absorption Ångström exponent (AAE, a), the mass absorption efficiency at 365 nm (MAE_{365}, b) in the water-soluble organic carbon (WSOC) and methanol-soluble organic carbon (MSOC) in aerosols samples from Bangkok in Thailand during 2016–2017.

The MAE at 365 nm (MAE_{365}) of the WSOC was 0.83±0.25 m^2 g^{-1} C, which was higher than that of the MSOC (0.26±0.12 m^2 g^{-1} C), indicating that more water-soluble BrC with stronger light absorption capability could be extracted with ultrapure deionized water, whereas water-insoluble BrC is characterized by lower light absorption capability over Bangkok. These results were consistent with those from vehicular exhaust samples in our previous study, where MAE_{365} values of the WSOC (0.71±0.30 m^2 g^{-1} C) were higher than those of the MSOC (0.26±0.09 m^2 g^{-1} C) (Tang et al., 2020b). Opposite results have been shown for primary biomass burning and coal combustion (Tang et al., 2020b). Similarly, Bikkina et al. (2020) observed that the marine-impacted aerosols of the Bay of

Bengal showed higher MAE_{365} values in the WSOC fraction than MSOC fraction (only extract using methanol), and they explained it due to two plausible reasons. First, the BrC aerosols over Bay of Bengal have a contribution from a different source (i.e., maritime influence) and contain BrC-chromophores that are more soluble in water than methanol. Secondary, there could be significant photobleaching effects of different chromophores. However, Wu et al. (2020b) reported that the MAE_{365} values of methanol-extracts are higher than those of WSOC in winter, whereas the situation is reversed in summer. Therefore, we infer that the different sources and atmospheric processes would impact the distribution of water-soluble and methanol-soluble chromophores. Considering the high temperature and humidity (Table S1), and tropical monsoon climate in Thailand, it seems to promote more water-soluble chromophores over Thailand. As not all water-insoluble components can be extracted with methanol, the observed light absorption by MSOC would therefore likely reflect the lower limit. Table S3 shows a comparison of the MAE values of Bangkok aerosols with those of other regions, indicating a medium light absorption capacity. The MAE_{365} values of the water-soluble fraction in this study were comparable to those of Nanjing (Chen et al., 2018), Guangzhou (Liu et al., 2018), and Beijing in summer (Yan et al., 2015), but lower than those of $PM_{2.5}$ from Singapore (Adam et al., 2020), PM_{10} from Godavari, Nepal, in the pre-monsoon season (Wu et al., 2019), and smoke particles from biomass burning and coal combustion (Park and Yu, 2016;Fan et al., 2018;Tang et al., 2020b). Lower MAE_{365} values of both fractions were observed in the monsoon season than in the non-monsoon seasons, likely due to the heavy monsoon rains that effectively remove soluble gases and aerosols (Lawrence and Lelieveld, 2010) and/or reduce biomass-burning activity (levoglucosan level in Table 1). A previous study reported similar findings in the USA in that the MAE_{365} was approximately three-fold higher in biomass burning-impacted samples than in non-biomass burning-impacted samples (Hecobian et al., 2010). Another study in the central Tibetan Plateau highlighted that BrC emitted by biomass burning has stronger light absorption capability than does secondary BrC formed in the atmosphere (Wu et al., 2018). On the Indo-China peninsula, Bangkok receives 99% of the fire-derived aerosols from December to April (Lee et al., 2017), which may explain the high absorption levels in the non-monsoon seasons.

3.4. Chromophores responsible for BrC light absorption.

EEM analysis enables the probing of the chemical structure of DOM because of its ability to distinguish among different classes of organic matter (Wu et al., 2003). Generally, BrC absorption is related to the chromophores within it and is susceptible to change with variations in chemical properties, e.g., oxidation level (Mo et al., 2018), degree of unsaturation (Jiang et al., 2020), molecular weight (Tang et al., 2020b;Di Lorenzo et al., 2017), functional groups (Chen et al., 2017b), molecular

composition, etc (Song et al., 2019;Lin et al., 2018). The fluorescence intensity of each EEM component was shown to be associated with light absorption indices, such as MAE_{365} and AAE, of HULIS in controlled crop straw-combustion experiments (Huo et al., 2018). As a linear relationship between organic matter concentration and fluorescence intensity can be assumed for very dilute samples due to the IFE (Murphy et al., 2013), we have corrected our fluorescence data for IFE using absorbance to enable "clean " correlation analysis (as shown in Fig. S13 a, b). The linear regression slopes in the scatter plots of Abs_{365} versus WSOC or MSOC could mathematically represent the average MAE values of WSOC or MSOC at 365 nm, respectively (Fig. S11 a, b). The phenomenon indicates that both fluorescence and Abs_{365} data point to similar relationships between sources or chemical processes with organic matter concentrations, and therefore, we attempted to link the fluorescence results to BrC absorption. It should be noted that light-absorbing substances in atmospheric particulate matter are not necessarily all fluorescent, such as nitrophenol compounds, which are a type of BrC commonly found in the atmospheric particulate matter; however, there is no strong fluorescence signal with which to scan the nitrophenol standards (Chen et al., 2019a).

In order to evaluate the light absorption from different fluorescent chromophores, we used MLR to explore the relationship between the fluorescence intensities of chromophores and Abs_{365}. In this study, light absorption properties were treated as the dependent variables, and the fluorescence were independent variables. During MLR, insignificant fluorescent components were excluded from the regression using a stepwise screening process to avoid overfitting ($F_{inclusion}$: $p < 0.05$; $F_{elimination}$: $p > 0.10$). The MLR statistical metrics are listed in Tables S4 and S5. For the independent variables with significant correlations with the dependent variable ($p < 0.05$), or with positive contributions to the independence, Abs_{365}, they will be retained in the statistical model as the efficiency factors to Abs_{365}. Thus, for the WSOC fraction, a revised model (regression 3) equation was used with an adjusted R^2 of 0.995. The final optimized equations were $Abs_{365} = 0.765 \times P4 + 0.051 \times P2 + 0.091 \times P7$, for the WSOC fraction, and $Abs_{365} = 0.238 \times C4$ for the MSOC fraction (Table S5). The model errors for water-soluble and methanol-soluble Abs_{365} were −5.5%–64% and −34%–58%, respectively. The predicted Abs_{365} values fit the measured values well (Fig. 5, slope = 0.99 and 0.95, and R^2 = 0.99 and 0.94 for WSOC and MSOC, respectively).

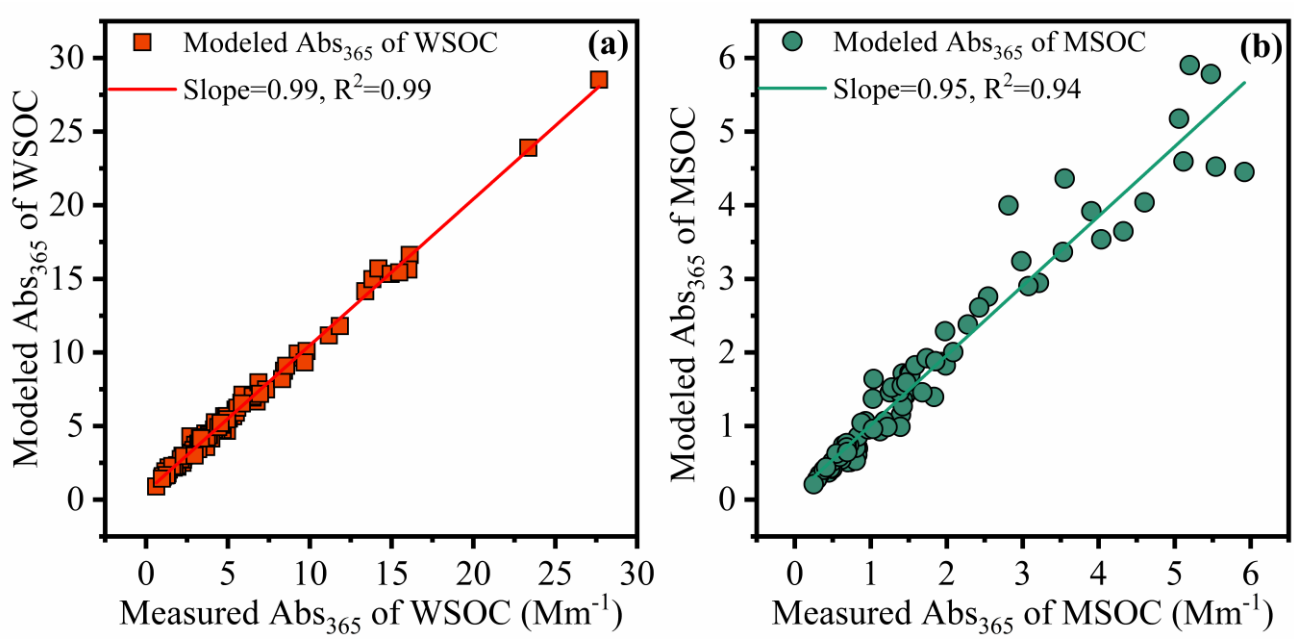

Figure 5. Linear correlation analysis between modeling Abs_{365} using multiple linear regression (MLR) analysis and measured Abs_{365} in the water-soluble organic carbon (WSOC, a) and methanol-soluble organic carbon (MSOC, b) in aerosols samples from Bangkok in Thailand during 2016–2017, respectively. Note that the fluorescent intensities of parallel factor (PARAFAC) model results (fluorescent components) were used as variables in MLR analysis.

For water-soluble BrC, the P4 component had the largest coefficient with Abs_{365}, which was much higher than those for P2 and P7. The C4 component had the largest coefficient with Abs_{365} for methanol-soluble BrC. These results indicate that the light absorption by BrC is more dependent on chromophores with longer emission wavelengths (P4 and C4). These characteristics also indicate that the strongly absorbing substances in BrC probably originate from large conjugated electron functional groups or include donor and acceptor molecules for charge-transfer interactions (Del Vecchio and Blough, 2004;Cory and McKnight, 2005). Kellerman et al. (2015) reported that these components are highly aromatic and oxygen-rich with high apparent molecular weight. These important findings highlight that larger chromophores may be the most persistent BrC species in the atmosphere and hence exert the greatest influence for perturbing the global radiative balance.

To further interpret the BrC source profiles as real-world TSP sources, we examined 84 (minus one missing value) TSP samples from Bangkok using the US EPA PMF5.0 model. All samples were merged together to form an 84 × 30 dataset (84 samples with 30 species). The initial data of positive matrix factorization input were from our previous study (Wang et al., 2020a). We further added Abs_{365} values of WSOC and MSOC, and the fluorescence intensities (in RU) of P2, P4, P7, and C4 components to the model. A seven-factor solution was achieved that provided the most physically reasonable source profiles (Fig. S14), including ship emission, secondary sulfate, dust, land fossil-fuel combustion, sea salt, biomass burning, and industrial emission, consistent with our previous study

(Wang et al., 2020a). Figure S15 shows the contributions of the above sources to light absorption at λ= 365 nm, which represent the fraction of BrC for each factor. Biomass burning was found to be the main source of BrC over Bangkok; 58% and 74% for water-soluble and methanol-soluble BrC, respectively. These were comparable to previous observations using a similar approach in Xi'an (55%) (Wu et al., 2020a). The time-series of Abs_{365} of WSOC and MSOC contributed by factors shows the high biomass burning contribution is related to the higher local fire spots (i.e., pre-hot season, hot season, and cool season) and/or air mass from the continent (Fig. S16–S17). Jiang et al. (2021) observed increases in biomass burning contributions to BrC absorption during the winter period that was dominant in continental-origin air masses. Furthermore, the P4 and C4 components, which were more closely associated with Abs_{365}, could be mostly attributed to biomass burning (54% and 70%, respectively) as shown in Fig. 6. Our previous study showed that biomass burning accounted for a considerably large portion (mean: 26%) of the TSP mass concentration in the same samples (Wang et al., 2020a). This result suggests that biomass burning makes a significant contribution to not only particulate matter but also BrC light absorption.

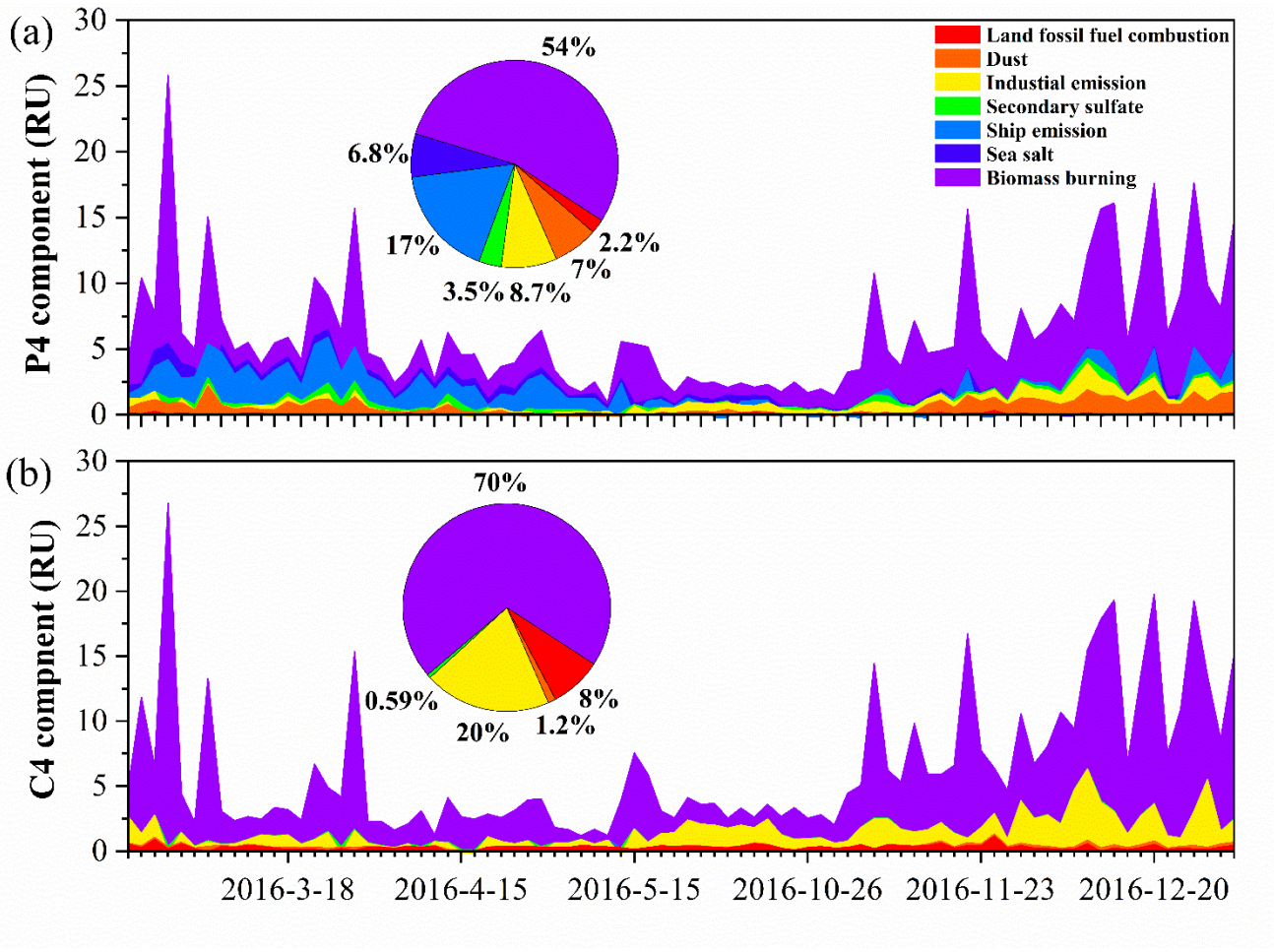

Figure 6. The time-series of P4 component of the WSOC (a) and C4 of the MSOC (b) in TSP samples over Bangkok in Thailand contributed by each factor resolved by positive matrix factorization.

4. Conclusions

This study presents a comprehensive analysis of water- and methanol-soluble chromophores in aerosol samples over Bangkok in Thailand during 2016–2017. EEM combining with PARAFAC analysis showed that the identified fluorescent components were humic-like and protein-like substances but different patterns in the WSOC and MSOC, indicating different chemical compositions. By adding three-source fluorescence into the original PARAFAC model, we found that chromophores with longer emission wavelengths in the atmosphere may be due to atmospheric chemical reactions or "aging" by both bleaching the source chromophores or producing new chromophores. We also suggest that caution is required when using fluorescence indices to appoint source of atmospheric chromophores. In addition, more water-soluble BrC with stronger light absorption capability could be extracted with ultrapure deionized water over Bangkok (0.83±0.25 vs. 0.26±0.12 m^2 g^{-1} C), and both water-soluble and methanol-soluble BrC exhibited a high light-absorption in non-monsoon seasons due to the influence of biomass burning. The MLR analysis showed that both the light absorption of BrC at 365 nm in the two fractions was significantly dependent on the special fluorescent chromophores with longer emission wavelength that are generally highly aromatic and oxygen-rich with high apparent molecular weight. Positive matrix factorization model results further showed that biomass burning was main contributor of these fluorescent chromophores (up to 50%). In summary, this study provides a new insight into BrC absorption and sources, which may promote the application of EEM spectroscopy to predict and model the light absorption of BrC in the atmosphere.

Data availability. The data used in this study are available upon request. Please contact Guangcai Zhong (gczhong@gig.ac.cn).

Supplement. The supplement related to this article is available.

Author contributions. JT, GZ, JL, and GZ (Guangcai Zhong) designed the experiment. JT and JW carried out the measurements and analyzed the data. JW and SB organized and performed the samplings. JT (Jianhui Tang) supported the fluorescence instruments and laboratory. CT and HJ supported the models. JT wrote the paper. JL, GZ (Guangcai Zhong), YC, YM, BZ, XG, and GZ reviewed and commented on the paper.

Competing interests. The authors declare that they have no conflict of interest.

Acknowledgements: This research has been supported by the National Natural Science Foundation of China (42030715, 41430645 and 41773120), the International Partnership Program of Chinese

Academy of Sciences (grant no. 132744KYSB20170002), Guangdong Foundation for Program of Science and Technology Research (Grant Nos. 2017BT01Z134, 2018A030310022, 2019B121205006, and 2020B1212060053), and China Postdoctoral Science Foundation (2020M682937).

References

Adam, M. G., Chiang, A. W. J., and Balasubramanian, R.: Insights into characteristics of light absorbing carbonaceous aerosols over an urban location in Southeast Asia, Environ. Pollut., 257, 113425, https://doi.org/10.1016/j.envpol.2019.113425, 2020.

Alexander, D. T. L., Crozier, P. A., and Anderson, J. R.: Brown carbon spheres in East Asian outflow and their optical properties, Science, 321, 833-836, https://doi.org/10.1126/science.1155296, 2008.

Andersson, C. A., and Bro, R.: The N-way Toolbox for MATLAB, Chemom. Intell. Lab. Syst., 52, 1-4, https://doi.org/10.1016/s0169-7439(00)00071-x, 2000.

Babar, Z. B., Park, J.-H., and Lim, H.-J.: Influence of NH 3 on secondary organic aerosols from the ozonolysis and photooxidation of α-pinene in a flow reactor, Atmos. Environ., 164, 71-84, https://doi.org/10.1016/j.atmosenv.2017.05.034, 2017.

Bahram, M., Bro, R., Stedmon, C., and Afkhami, A.: Handling of Rayleigh and Raman scatter for PARAFAC modeling of fluorescence data using interpolation, J. Chemom., 20, 99-105, https://doi.org/10.1002/cem.978, 2006.

Barnard, J. C., Volkamer, R., and Kassianov, E. I.: Estimation of the mass absorption cross section of the organic carbon component of aerosols in the Mexico City Metropolitan Area, Atmos. Chem. Phys., 8, 6665-6679, http://doi.org/10.5194/acp-8-6665-2008, 2008.

Bianco, A., Minella, M., De Laurentiis, E., Maurino, V., Minero, C., and Vione, D.: Photochemical generation of photoactive compounds with fulvic-like and humic-like fluorescence in aqueous solution, Chemosphere, 111, 529-536, https://doi.org/10.1016/j.chemosphere.2014.04.035, 2014.

Bianco, A., Passananti, M., Deguillaume, L., Mailhot, G., and Brigante, M.: Tryptophan and tryptophan-like substances in cloud water: Occurrence and photochemical fate, Atmos. Environ., 137, 53-61, https://doi.org/10.1016/j.atmosenv.2016.04.034, 2016.

Bikkina, P., Bikkina, S., Kawamura, K., Sudheer, A. K., Mahesh, G., and Kumar, S. K.: Evidence for brown carbon absorption over the Bay of Bengal during the southwest monsoon season: a possible oceanic source, Environ Sci Process Impacts, 22, 1743-1758, https://doi.org/10.1039/d0em00111b, 2020.

Birdwell, J. E., and Engel, A. S.: Characterization of dissolved organic matter in cave and spring waters using UV–Vis absorbance and fluorescence spectroscopy, Org. Geochem., 41, 270-280, https://doi.org/10.1016/j.orggeochem.2009.11.002, 2010.

Birdwell, J. E., and Valsaraj, K. T.: Characterization of dissolved organic matter in fogwater by excitation–emission matrix fluorescence spectroscopy, Atmos. Environ., 44, 3246-3253, https://doi.org/10.1016/j.atmosenv.2010.05.055, 2010.

Chen, H., Liao, Z. L., Gu, X. Y., Xie, J. Q., Li, H. Z., and Zhang, J.: Anthropogenic Influences of Paved Runoff and Sanitary Sewage on the Dissolved Organic Matter Quality of Wet Weather Overflows: An Excitation-Emission

Matrix Parallel Factor Analysis Assessment, Environ. Sci. Technol., 51, 1157-1167, https://doi.org/10.1021/acs.est.6b03727, 2017a.

Chen, Q., Ikemori, F., and Mochida, M.: Light Absorption and Excitation-Emission Fluorescence of Urban Organic Aerosol Components and Their Relationship to Chemical Structure, Environ. Sci. Technol., 50, 10859-10868, https://doi.org/10.1021/acs.est.6b02541, 2016a.

Chen, Q., Miyazaki, Y., Kawamura, K., Matsumoto, K., Coburn, S., Volkamer, R., Iwamoto, Y., Kagami, S., Deng, Y., Ogawa, S., Ramasamy, S., Kato, S., Ida, A., Kajii, Y., and Mochida, M.: Characterization of Chromophoric Water-Soluble Organic Matter in Urban, Forest, and Marine Aerosols by HR-ToF-AMS Analysis and Excitation-Emission Matrix Spectroscopy, Environ. Sci. Technol., 50, 10351-10360, https://doi.org/10.1021/acs.est.6b01643, 2016b.

Chen, Q., Ikemori, F., Nakamura, Y., Vodicka, P., Kawamura, K., and Mochida, M.: Structural and Light-Absorption Characteristics of Complex Water-Insoluble Organic Mixtures in Urban Submicrometer Aerosols, Environ. Sci. Technol., 51, 8293-8303, https://doi.org/10.1021/acs.est.7b01630., 2017b.

Chen, Q., Mu, Z., Song, W., Wang, Y., Yang, Z., Zhang, L., and Zhang, Y. L.: Size‐Resolved Characterization of the Chromophores in Atmospheric Particulate Matter From a Typical Coal-Burning City in China, J. Geophys. Res.-Atmos., 124, 10546-10563, https://doi.org/10.1029/2019jd031149, 2019a.

Chen, Q., Wang, M., Wang, Y., Zhang, L., Li, Y., and Han, Y.: Oxidative Potential of Water-Soluble Matter Associated with Chromophoric Substances in PM2.5 over Xi'an, China, Environ. Sci. Technol., 53, 8574-8584, https://doi.org/10.1021/acs.est.9b01976, 2019b.

Chen, W., Westerhoff, P., Leenheer, J. A., and Booksh, K.: Fluorescence excitation - Emission matrix regional integration to quantify spectra for dissolved organic matter, Environ. Sci. Technol., 37, 5701-5710, https://doi.org/10.1021/es034354c 2003.

Chen, Y., and Bond, T. C.: Light absorption by organic carbon from wood combustion, Atmos. Chem. Phys., 10, 1773-1787, https://doi.org/10.5194/acp-10-1773-2010, 2010.

Chen, Y., Ge, X., Chen, H., Xie, X., Chen, Y., Wang, J., Ye, Z., Bao, M., Zhang, Y., and Chen, M.: Seasonal light absorption properties of water-soluble brown carbon in atmospheric fine particles in Nanjing, China, Atmos. Environ., 230-240, https://doi.org/10.1016/j.atmosenv.2018.06.002, 2018.

Cory, R. M., and McKnight, D. M.: Fluorescence spectroscopy reveals ubiquitous presence of oxidized and reduced quinones in dissolved organic matter, Environ. Sci. Technol., 39, 8142-8149, https://doi.org/10.1021/es0506962, 2005.

Dasari, S., Andersson, A., Bikkina, S., Holmstrand, H., Budhavant, K., Satheesh, S., Asmi, E., Kesti, J., Backman, J., Salam, A., Bisht, D. S., Tiwari, S., Hameed, Z., and Gustafsson, O.: Photochemical degradation affects the light absorption of water-soluble brown carbon in the South Asian outflow, Sci. Adv., 5, 10, https://doi.org/10.1126/sciadv.aau8066, 2019.

Del Vecchio, R., and Blough, N. V.: On the Origin of the Optical Properties of Humic Substances, Environ. Sci. Technol., 38, 3885-3891, https://doi.org/10.1021/es049912h, 2004.

Di Lorenzo, R. A., Washenfelder, R. A., Attwood, A. R., Guo, H., Xu, L., Ng, N. L., Weber, R. J., Baumann, K., Edgerton, E., and Young, C. J.: Molecular-Size-Separated Brown Carbon Absorption for Biomass-Burning

Aerosol at Multiple Field Sites, Environ. Sci. Technol., 51, 3128-3137, https://doi.org/10.1021/acs.est.6b06160, 2017.

Fan, X., Li, M., Cao, T., Cheng, C., Li, F., Xie, Y., Wei, S., Song, J., and Peng, P. a.: Optical properties and oxidative potential of water- and alkaline-soluble brown carbon in smoke particles emitted from laboratory simulated biomass burning, Atmos. Environ., 194, 48-57, https://10.1016/j.atmosenv.2018.09.025, 2018.

Fan, X. J., Cao, T., Yu, X. F., Wang, Y., Xiao, X., Li, F. Y., Xie, Y., Ji, W. C., Song, J. Z., and Peng, P. A.: The evolutionary behavior of chromophoric brown carbon during ozone aging of fine particles from biomass burning, Atmos. Chem. Phys., 20, 4593-4605, https://10.5194/acp-20-4593-2020, 2020.

Fu, P., Kawamura, K., Chen, J., Qin, M., Ren, L., Sun, Y., Wang, Z., Barrie, L. A., Tachibana, E., Ding, A., and Yamashita, Y.: Fluorescent water-soluble organic aerosols in the High Arctic atmosphere, Sci Rep, 5, 9845, https://doi.org/10.1038/srep09845, 2015.

Fujii, Y., Iriana, W., Oda, M., Puriwigati, A., Tohno, S., Lestari, P., Mizohata, A., and Huboyo, H. S.: Characteristics of carbonaceous aerosols emitted from peatland fire in Riau, Sumatra, Indonesia, Atmos. Environ., 87, 164-169, https://doi.org/10.1016/j.atmosenv.2014.01.037, 2014.

Gabor, R. S., Baker, A., McKnight, D. M., and Miller, M. P.: Fluorescence Indices and Their Interpretation, in: Aquatic Organic Matter Fluorescence, edited by: Baker, A., Reynolds, D. M., Lead, J., Coble, P. G., and Spencer, R. G. M., Cambridge Environmental Chemistry Series, Cambridge University Press, Cambridge, 303-338, 2014.

Gao, Y., and Zhang, Y.: Formation and photochemical investigation of brown carbon by hydroxyacetone reactions with glycine and ammonium sulfate, RSC Advances, 8, 20719-20725, https://doi.org/10.1039/c8ra02019a, 2018.

Graber, E. R., and Rudich, Y.: Atmospheric HULIS: How humic-like are they? A comprehensive and critical review, Atmos. Chem. Phys., 6, 729-753, https://doi.org/10.5194/acp-6-729-2006, 2006.

Gu, Q., and Kenny, J. E.: Improvement of Inner Filter Effect Correction Based on Determination of Effective Geometric Parameters Using a Conventional Fluorimeter, Anal. Chem., 81, 420-426, https://doi.org/10.1021/ac801676j, 2009.

Han, H., Kim, G., Seo, H., Shin, K.-H., and Lee, D.-H.: Significant seasonal changes in optical properties of brown carbon in the midlatitude atmosphere, Atmos. Chem. Phys., 20, 2709-2718, https://doi.org/10.5194/acp-20-2709-2020, 2020.

Hawkes, J. A., Patriarca, C., Sjöberg, P. J. R., Tranvik, L. J., and Bergquist, J.: Extreme isomeric complexity of dissolved organic matter found across aquatic environments, Limnol. Oceanogr. Lett., 3, 21-30, https://doi.org/10.1002/lol2.10064, 2018.

Hecobian, A., Zhang, X., Zheng, M., Frank, N., Edgerton, E. S., and Weber, R. J.: Water-Soluble Organic Aerosol material and the light-absorption characteristics of aqueous extracts measured over the Southeastern United States, Atmos. Chem. Phys., 10, 5965-5977, https://doi.org/10.5194/acp-10-5965-2010, 2010.

Hoffer, A., Gelencsér, A., Guyon, P., Kiss, G., Schmid, O., Frank, G., Artaxo, P., and Andreae, M.: Optical properties of humic-like substances (HULIS) in biomass-burning aerosols, Atmos. Chem. Phys., 6, 3563-3570, https://doi.org/10.5194/acp-6-3563-2006, 2006.

Hopkins, R. J., Lewis, K., Desyaterik, Y., Wang, Z., Tivanski, A. V., Arnott, W. P., Laskin, A., and Gilles, M. K.: Correlations between optical, chemical and physical properties of biomass burn aerosols, Geophys. Res. Lett.,

34, https://doi.org/10.1029/2007gl030502, 2007.

Huang, K., Fu, J. S., Hsu, N. C., Gao, Y., Dong, X., Tsay, S.-C., and Lam, Y. F.: Impact assessment of biomass burning on air quality in Southeast and East Asia during BASE-ASIA, Atmos. Environ., 78, 291-302, https://doi.org/10.1016/j.atmosenv.2012.03.048, 2013.

Huguet, A., Vacher, L., Relexans, S., Saubusse, S., Froidefond, J. M., and Parlanti, E.: Properties of fluorescent dissolved organic matter in the Gironde Estuary, Org. Geochem., 40, 706-719, https://doi.org/10.1016/j.orggeochem.2009.03.002, 2009.

Huo, Y., Li, M., Jiang, M., and Qi, W.: Light absorption properties of HULIS in primary particulate matter produced by crop straw combustion under different moisture contents and stacking modes, Atmos. Environ., 191, 490-499, https://doi.org/10.1016/j.atmosenv.2018.08.038, 2018.

Ishii, S. K., and Boyer, T. H.: Behavior of reoccurring PARAFAC components in fluorescent dissolved organic matter in natural and engineered systems: a critical review, Environ. Sci. Technol., 46, 2006-2017, https://doi.org/10.1021/es2043504, 2012.

Jiang, H., Li, J., Chen, D., Tang, J., Cheng, Z., Mo, Y., Su, T., Tian, C., Jiang, B., Liao, Y., and Zhang, G.: Biomass burning organic aerosols significantly influence the light absorption properties of polarity-dependent organic compounds in the Pearl River Delta Region, China, Environ. Int., 144, 106079, https://doi.org/10.1016/j.envint.2020.106079, 2020.

Jiang, H., Li, J., Sun, R., Liu, G., Tian, C., Tang, J., Cheng, Z., Zhu, S., Zhong, G., Ding, X., and Zhang, G.: Determining the Sources and Transport of Brown Carbon Using Radionuclide Tracers and Modeling, J. Geophys. Res.-Atmos., 126, https://doi.org/10.1029/2021jd034616, 2021.

Kasthuriarachchi, N. Y., Rivellini, L.-H., Chen, X., Li, Y. J., and Lee, A. K. Y.: Effect of relative humidity on secondary brown carbon formation in aqueous droplets, Environ. Sci. Technol., 54, 13207-13216, https://doi.org/10.1021/acs.est.0c01239, 2020.

Kellerman, A. M., Kothawala, D. N., Dittmar, T., and Tranvik, L. J.: Persistence of dissolved organic matter in lakes related to its molecular characteristics, Nat. Geosci., 8, 454-U452, https://doi.org/10.1038/ngeo2440, 2015.

Kirchstetter, T. W., Novakov, T., and Hobbs, P. V.: Evidence that the spectral dependence of light absorption by aerosols is affected by organic carbon, J. Geophys. Res.-Atmos., 109, https://doi.org/10.1029/2004jd004999, 2004.

Kirchstetter, T. W., and Thatcher, T. L.: Contribution of organic carbon to wood smoke particulate matter absorption of solar radiation, Atmos. Chem. Phys., 12, 5803-5816, https://doi.org/10.5194/acp-12-6067-2012, 2012.

Lack, D. A., Bahreini, R., Langridge, J. M., Gilman, J. B., and Middlebrook, A. M.: Brown carbon absorption linked to organic mass tracers in biomass burning particles, Atmos. Chem. Phys., 13, 2415-2422, https://doi.org/10.5194/acp-13-2415-2013, 2013.

Laskin, A., Laskin, J., and Nizkorodov, S. A.: Chemistry of atmospheric brown carbon, Chem. Rev., 115, 4335-4382, https://doi.org/10.1021/cr5006167, 2015.

Laskin, J., Laskin, A., and Nizkorodov, S. A.: Mass Spectrometry Analysis in Atmospheric Chemistry, Anal. Chem., 90, 166-189, https://doi.org/10.1021/acs.analchem.7b04249, 2018.

Lawrence, M. G., and Lelieveld, J.: Atmospheric pollutant outflow from southern Asia: a review, Atmos. Chem. Phys.,

10, 11017-11096, https://doi.org/10.5194/acp-10-11017-2010, 2010.

Lee, H.-H., Bar-Or, R. Z., and Wang, C.: Biomass burning aerosols and the low-visibility events in Southeast Asia, Atmos. Chem. Phys., 17, 965-980, https://doi.org/10.5194/acp-17-965-2017, 2017.

Lee, H. J., Laskin, A., Laskin, J., and Nizkorodov, S. A.: Excitation-emission spectra and fluorescence quantum yields for fresh and aged biogenic secondary organic aerosols, Environ. Sci. Technol., 47, 5763-5770, https://doi.org/10.1021/es400644c, 2013.

Li, M., Fan, X., Zhu, M., Zou, C., Song, J., Wei, S., Jia, W., and Peng, P.: Abundances and light absorption properties of brown carbon emitted from residential coal combustion in China, Environ. Sci. Technol., 53, 595-603, https://doi.org/10.1021/acs.est.8b05630, 2018.

Lin, P., Laskin, J., Nizkorodov, S. A., and Laskin, A.: Revealing Brown Carbon Chromophores Produced in Reactions of Methylglyoxal with Ammonium Sulfate, Environ. Sci. Technol., 49, 14257-14266, https://doi.org/10.1021/acs.est.5b03608, 2015.

Lin, P., Aiona, P. K., Li, Y., Shiraiwa, M., Laskin, J., Nizkorodov, S. A., and Laskin, A.: Molecular Characterization of Brown Carbon in Biomass Burning Aerosol Particles, Environ. Sci. Technol., 50, 11815-11824, https://doi.org/10.1021/acs.est.6b03024, 2016.

Lin, P., Bluvshtein, N., Rudich, Y., Nizkorodov, S. A., Laskin, J., and Laskin, A.: Molecular Chemistry of Atmospheric Brown Carbon Inferred from a Nationwide Biomass Burning Event, Environ. Sci. Technol., 51, 11561-11570, https://doi.org/10.1021/acs.est.7b02276, 2017.

Lin, P., Fleming, L. T., Nizkorodov, S. A., Laskin, J., and Laskin, A.: Comprehensive Molecular Characterization of Atmospheric Brown Carbon by High Resolution Mass Spectrometry with Electrospray and Atmospheric Pressure Photoionization, Anal. Chem., 90, 12493-12502, https://doi.org/10.1021/acs.analchem.8b02177, 2018.

Liu, J., Bergin, M., Guo, H., King, L., Kotra, N., Edgerton, E., and Weber, R. J.: Size-resolved measurements of brown carbon in water and methanol extracts and estimates of their contribution to ambient fine-particle light absorption, Atmos. Chem. Phys., 13, 12389-12404, https://doi.org/10.5194/acp-13-12389-2013, 2013.

Liu, J., Mo, Y., Ding, P., Li, J., Shen, C., and Zhang, G.: Dual carbon isotopes ((14)C and (13)C) and optical properties of WSOC and HULIS-C during winter in Guangzhou, China, Sci. Total Environ., 633, 1571-1578, https://doi.org/10.1016/j.scitotenv.2018.03.293, 2018.

Luciani, X., Mounier, S., Redon, R., and Bois, A.: A simple correction method of inner filter effects affecting FEEM and its application to the PARAFAC decomposition, Chemom. Intell. Lab. Syst., 96, 227-238, https://doi.org/10.1016/j.chemolab.2009.02.008, 2009.

Marrero-Ortiz, W., Hu, M., Du, Z., Ji, Y., Wang, Y., Guo, S., Lin, Y., Gomez-Hermandez, M., Peng, J., Li, Y., Secrest, J., Levy Zamora, M., Wang, Y., An, T., and Zhang, R.: Formation and optical properties of brown carbon from small alpha-dicarbonyls and amines, Environ. Sci. Technol., https://doi.org/10.1021/acs.est.8b03995, 2018.

Matos, J. T. V., Freire, S. M. S. C., Duarte, R. M. B. O., and Duarte, A. C.: Natural organic matter in urban aerosols: Comparison between water and alkaline soluble components using excitation–emission matrix fluorescence spectroscopy and multiway data analysis, Atmos. Environ., 102, 1-10, https://doi.org/10.1016/j.atmosenv.2014.11.042, 2015.

Mcknight, D. M., Boyer, E. W., Westerhoff, P., Doran, P. T., Kulbe, T., and Andersen, D. T.: Spectrofluorometric

characterization of dissolved organic matter for indication of precursor organic material and aromaticity, Limnol. Oceanogr., 46, 38-48, https://doi.org/10.4319/lo.2001.46.1.0038, 2001.

Mo, Y., Li, J., Jiang, B., Su, T., Geng, X., Liu, J., Jiang, H., Shen, C., Ding, P., Zhong, G., Cheng, Z., Liao, Y., Tian, C., Chen, Y., and Zhang, G.: Sources, compositions, and optical properties of humic-like substances in Beijing during the 2014 APEC summit: Results from dual carbon isotope and Fourier-transform ion cyclotron resonance mass spectrometry analyses, Environ. Pollut., 239, 322-331, https://doi.org/10.1016/j.envpol.2018.04.041, 2018.

Mo, Y. Z., Li, J., Liu, J. W., Zhong, G. C., Cheng, Z. N., Tian, C. G., Chen, Y. J., and Zhang, G.: The influence of solvent and pH on determination of the light absorption properties of water-soluble brown carbon, Atmos. Environ., 161, 90-98, https://doi.org/10.1016/j.atmosenv.2017.04.037, 2017.

Mounier, S., Patel, N., Quilici, L., Benaim, J. Y., and Benamou, C.: Fluorescence 3D de la matière organique dissoute du fleuve amazone: (Three-dimensional fluorescence of the dissolved organic carbon in the Amazon river), Water Res., 33, 1523-1533, https://doi.org/10.1016/S0043-1354(98)00347-9, 1999.

Murphy, K. R., Butler, K. D., Spencer, R. G., Stedmon, C. A., Boehme, J. R., and Aiken, G. R.: Measurement of dissolved organic matter fluorescence in aquatic environments: an interlaboratory comparison, Environ. Sci. Technol., 44, 9405-9412, https://doi.org/10.1021/es102362t, 2010.

Murphy, K. R., Stedmon, C. A., Graeber, D., and Bro, R.: Fluorescence spectroscopy and multi-way techniques. PARAFAC, Anal. Methods, 5, 6557-6566, https://doi.org/10.1039/c3ay41160e, 2013.

Murphy, K. R., Timko, S. A., Gonsior, M., Powers, L. C., Wunsch, U. J., and Stedmon, C. A.: Photochemistry Illuminates Ubiquitous Organic Matter Fluorescence Spectra, Environ. Sci. Technol., 52, 11243-11250, https://doi.org/10.1021/acs.est.8b02648, 2018.

Park, S. S., and Yu, J.: Chemical and light absorption properties of humic-like substances from biomass burning emissions under controlled combustion experiments, Atmos. Environ., 136, 114-122, https://doi.org/10.1016/j.atmosenv.2016.04.022, 2016.

Permadi, D. A., Kim Oanh, N. T., and Vautard, R.: Assessment of emission scenarios for 2030 and impacts of black carbon emission reduction measures on air quality and radiative forcing in Southeast Asia, Atmos. Chem. Phys., 18, 3321-3334, https://doi.org/10.5194/acp-18-3321-2018, 2018.

Pohlker, C., Huffman, J. A., and Poschl, U.: Autofluorescence of atmospheric bioaerosols – fluorescent biomolecules and potential interferences, Atmos. Meas. Tech., 5, 37-71, https://doi.org/10.5194/amt-5-37-2012, 2012.

Qin, J., Zhang, L., Zhou, X., Duan, J., Mu, S., Xiao, K., Hu, J., and Tan, J.: Fluorescence fingerprinting properties for exploring water-soluble organic compounds in $PM_{2.5}$ in an industrial city of northwest China, Atmos. Environ., 184, 203-211, https://doi.org/10.1016/j.atmosenv.2018.04.049, 2018.

Ramanathan, V., Li, F., Ramana, M. V., Praveen, P. S., Kim, D., Corrigan, C. E., Van Nguyen, H., Stone, E. A., Schauer, J. J., and Carmichael, G. R.: Atmospheric brown clouds: Hemispherical and regional variations in long-range transport, absorption, and radiative forcing, J. Geophys. Res., 112, https://doi.org/10.1029/2006JD008124, 2007.

See, S. W., Balasubramanian, R., and Wang, W.: A study of the physical, chemical, and optical properties of ambient aerosol particles in Southeast Asia during hazy and nonhazy days, J. Geophys. Res.-Atmos., 111, https://doi.org/10.1029/2005JD006180, 2006.

Shimabuku, K. K., Kennedy, A. M., Mulhern, R. E., and Summers, R. S.: Evaluating Activated Carbon Adsorption of Dissolved Organic Matter and Micropollutants Using Fluorescence Spectroscopy, Environ. Sci. Technol., 51, 2676-2684, https://doi.org/10.1021/acs.est.6b04911, 2017.

Song, J., Li, M., Jiang, B., Wei, S., Fan, X., and Peng, P.: Molecular Characterization of Water-Soluble Humic like Substances in Smoke Particles Emitted from Combustion of Biomass Materials and Coal Using Ultrahigh-Resolution Electrospray Ionization Fourier Transform Ion Cyclotron Resonance Mass Spectrometry, Environ. Sci. Technol., 52, 2575-2585, https://doi.org/10.1021/acs.est.7b06126, 2018.

Song, J. Z., Li, M. J., Fan, X. J., Zou, C. L., Zhu, M. B., Jiang, B., Yu, Z. Q., Jia, W. L., Liao, Y. H., and Peng, P. A.: Molecular Characterization of Water- and Methanol-Soluble Organic Compounds Emitted from Residential Coal Combustion Using Ultrahigh-Resolution Electrospray Ionization Fourier Transform Ion Cyclotron Resonance Mass Spectrometry, Environ. Sci. Technol., 53, 13607-13617, https://doi.org/10.1021/acs.est.9b04331, 2019.

Stedmon, C. A., and Markager, S.: Resolving the variability in dissolved organic matter fluorescence in a temperate estuary and its catchment using PARAFAC analysis, Limnol. Oceanogr., 50, 686-697, https://doi.org/10.4319/lo.2005.50.2.0686, 2005.

Tang, J., Li, J., Mo, Y., Safaei Khorram, M., Chen, Y., Tang, J., Zhang, Y., Song, J., and Zhang, G.: Light absorption and emissions inventory of humic-like substances from simulated rainforest biomass burning in Southeast Asia, Environ. Pollut., 262, 114266, https://doi.org/10.1016/j.envpol.2020.114266, 2020a.

Tang, J., Li, J., Su, T., Han, Y., Mo, Y., Jiang, H., Cui, M., Jiang, B., Chen, Y., Tang, J., Song, J., Peng, P., and Zhang, G.: Molecular compositions and optical properties of dissolved brown carbon in biomass burning, coal combustion, and vehicle emission aerosols illuminated by excitation–emission matrix spectroscopy and Fourier transform ion cyclotron resonance mass spectrometry analysis, Atmos. Chem. Phys., 20, 2513-2532, https://doi.org/10.5194/acp-20-2513-2020, 2020b.

Wang, J., Jiang, H., Jiang, H., Mo, Y., Geng, X., Li, J., Mao, S., Bualert, S., Ma, S., Li, J., and Zhang, G.: Source apportionment of water-soluble oxidative potential in ambient total suspended particulate from Bangkok: Biomass burning versus fossil fuel combustion, Atmos. Environ., 235, 117624, https://doi.org/10.1016/j.atmosenv.2020.117624, 2020a.

Wang, K., Pang, Y., He, C., Li, P., Xiao, S., Sun, Y., Pan, Q., Zhang, Y., Shi, Q., and He, D.: Optical and molecular signatures of dissolved organic matter in Xiangxi Bay and mainstream of Three Gorges Reservoir, China: Spatial variations and environmental implications, Sci. Total Environ., 657, 1274-1284, https://doi.org/10.1016/j.scitotenv.2018.12.117, 2019.

Wang, X., Hayeck, N., Brüggemann, M., Abis, L., Riva, M., Lu, Y., Wang, B., Chen, J., George, C., and Wang, L.: Chemical Characteristics and Brown Carbon Chromophores of Atmospheric Organic Aerosols Over the Yangtze River Channel: A Cruise Campaign, J. Geophys. Res.-Atmos., 125, e2020JD032497, https://doi.org/10.1029/2020jd032497, 2020b.

Wong, J. P. S., Nenes, A., and Weber, R. J.: Changes in Light Absorptivity of Molecular Weight Separated Brown Carbon Due to Photolytic Aging, Environ. Sci. Technol., 51, 8414-8421, https://doi.org/10.1021/acs.est.7b01739, 2017.

Wu, C., Wang, G., Li, J., Li, J., Cao, C., Ge, S., Xie, Y., Chen, J., Li, X., Xue, G., Wang, X., Zhao, Z., and Cao, F.: The characteristics of atmospheric brown carbon in Xi'an, inland China: sources, size distributions and optical properties, Atmos. Chem. Phys., 20, 2017-2030, https://doi.org/10.5194/acp-20-2017-2020, 2020a.

Wu, F. C., Evans, R. D., and Dillon, P. J.: Separation and Characterization of NOM by High-Performance Liquid Chromatography and On-Line Three-Dimensional Excitation Emission Matrix Fluorescence Detection, Environ. Sci. Technol., 37, 3687-3693, https://doi.org/10.1021/es020244e, 2003.

Wu, G., Wan, X., Gao, S., Fu, P., Yin, Y., Li, G., Zhang, G., Kang, S., Ram, K., and Cong, Z.: Humic-Like Substances (HULIS) in Aerosols of Central Tibetan Plateau (Nam Co, 4730 m asl): Abundance, Light Absorption Properties, and Sources, Environ. Sci. Technol., 52, 7203-7211, https://doi.org/10.1021/acs.est.8b01251, 2018.

Wu, G., Ram, K., Fu, P., Wang, W., Zhang, Y., Liu, X., Stone, E. A., Pradhan, B. B., Dangol, P. M., Panday, A. K., Wan, X., Bai, Z., Kang, S., Zhang, Q., and Cong, Z.: Water-Soluble Brown Carbon in Atmospheric Aerosols from Godavari (Nepal), a Regional Representative of South Asia, Environ. Sci. Technol., 53, 3471-3479, https://doi.org/10.1021/acs.est.9b00596, 2019.

Wu, G., Wan, X., Ram, K., Li, P., Liu, B., Yin, Y., Fu, P., Loewen, M., Gao, S., Kang, S., Kawamura, K., Wang, Y., and Cong, Z.: Light absorption, fluorescence properties and sources of brown carbon aerosols in the Southeast Tibetan Plateau, Environ. Pollut., 257, 113616, https://doi.org/10.1016/j.envpol.2019.113616, 2020b.

Wu, G., Fu, P., Ram, K., Song, J., Chen, Q., Kawamura, K., Wan, X., Kang, S., Wang, X., Laskin, A., and Cong, Z.: Fluorescence characteristics of water-soluble organic carbon in atmospheric aerosol, Environ. Pollut., 268, 115906, https://doi.org/10.1016/j.envpol.2020.115906, 2021.

Xie, M., Chen, X., Holder, A. L., Hays, M. D., Lewandowski, M., Offenberg, J. H., Kleindienst, T. E., Jaoui, M., and Hannigan, M. P.: Light absorption of organic carbon and its sources at a southeastern U.S. location in summer, Environ. Pollut., 244, 38-46, https://doi.org/10.1016/j.envpol.2018.09.125, 2019.

Yan, C., Zheng, M., Sullivan, A. P., Bosch, C., Desyaterik, Y., Andersson, A., Li, X., Guo, X., Zhou, T., Gustafsson, Ö., and Collett, J. L.: Chemical characteristics and light-absorbing property of water-soluble organic carbon in Beijing: Biomass burning contributions, Atmos. Environ., 121, 4-12, https://doi.org/10.1016/j.atmosenv.2015.05.005, 2015.

Yan, C., Zheng, M., Desyaterik, Y., Sullivan, A. P., Wu, Y., and Collett Jr., J. L.: Molecular Characterization of Water-Soluble Brown Carbon Chromophores in Beijing, China, J. Geophys. Res.-Atmos., 125, e2019JD032018, https://doi.org/10.1029/2019jd032018, 2020.

Yan, G., and Kim, G.: Speciation and Sources of Brown Carbon in Precipitation at Seoul, Korea: Insights from Excitation-Emission Matrix Spectroscopy and Carbon Isotopic Analysis, Environ. Sci. Technol., 51, 11580-11587, https://doi.org/10.1021/acs.est.7b02892, 2017.

Yue, S., Ren, L., Song, T., Li, L., Xie, Q., Li, W., Kang, M., Zhao, W., Wei, L., Ren, H., Sun, Y., Wang, Z., Ellam, R. M., Liu, C. Q., Kawamura, K., and Fu, P.: Abundance and Diurnal Trends of Fluorescent Bioaerosols in the Troposphere over Mt. Tai, China, in Spring, J. Geophys. Res.-Atmos., 124, 4158-4173, https://doi.org/10.1029/2018jd029486, 2019.

Zhou, Y., Wen, H., Liu, J., Pu, W., Chen, Q., and Wang, X.: The optical characteristics and sources of chromophoric dissolved organic matter (CDOM) in seasonal snow of northwestern China, The Cryosphere, 13, 157-175,

https://doi.org/10.5194/tc-13-157-2019, 2019.

Zsolnay, A., Baigar, E., Jimenez, M., Steinweg, B., and Saccomandi, F.: Differentiating with fluorescence spectroscopy the sources of dissolved organic matter in soils subjected to drying, Chemosphere, 38, 45-50, https://doi.org/10.1016/S0045-6535(98)00166-0, 1999.